MSDE

ROYAL SOCIETY OF CHEMISTRY

MINI REVIEW

View Article Online
View Journal | View Issue

Cite this: *Mol. Syst. Des. Eng.*, 2022, 7, 1588

Recent advances in molecular programming of liquid crystal elastomers with additive manufacturing for 4D printing

Yueping Wang,[a] Jongwon An[b] and Howon Lee *[b]

Received 27th June 2022,
Accepted 14th September 2022

DOI: 10.1039/d2me00124a

rsc.li/molecular-engineering

Liquid crystal elastomers (LCEs) are crosslinked polymers within which liquid crystal molecules are linked with elastomeric polymer chains. Various anisotropic materials properties of LCEs can be created through an orientational control of mesogens during the fabrication process. In particular, LCEs exhibit reversible mechanical deformation along the direction of mesogen alignment in response to various external stimuli. Therefore, when properly associated with a suitable additive manufacturing process, LCEs can be fabricated into a 3D object that displays programmed stimuli-responsive deformation. Thus, LCEs offer a potential breakthrough in 4D printing as an alternative material solution that overcomes the limitations of typical 4D printing materials such as shape memory polymers and hydrogels. The orientational order of mesogens in LCEs can be controlled by a wide range of methods, including mechanical stretch, viscous shear flow, magnetic/electric-field, and surface treatment. We review herein the physical principles of the key methods for LCE molecular programming and recent advances in additive manufacturing processes that utilize these principles to enable 4D printing with LCEs. Various applications of additively manufactured LCEs are also highlighted.

Design, System, Application

Time is the 4th dimension in 4D printing. With the unprecedented interplay of materials science and additive manufacturing (AM), 4D-printed objects are able to change shape and property in response to external stimuli such as temperature and light. Advances in materials science, in particular, have played a crucial role in the emergence of 4D printing by providing fundamental understanding for time-dependent deformation of printed materials. While shape memory polymers and hydrogels are the first-generation materials in 4D printing, attention has recently been rapidly shifting to liquid crystal elastomers (LCEs). LCEs are crosslinked polymers within which liquid crystal molecules are linked with elastomeric polymer chains. With the recent progresses in AM, LCEs have been rapidly expanding their reach across a broad spectrum of application sectors. Since the morphing of LCE is dictated by the prescribed orientations of the mesogens, recent research has focused heavily on encoding the molecular order of mesogens in 3D printed LCEs. We review herein the physical principles underlying the key methods for LCE molecular programming and recent advances in AM processes that utilize these principles for LCE 4D printing. Various applications of additively manufactured LCEs are also highlighted.

1. Introduction

Programmable matter that can actively deform and reconfigure when exposed to external inputs has been extensively studied for its strong potential for intelligent and adaptive material systems. Additive manufacturing with such materials is referred to as 4D printing, with the fourth dimension being time. By using stimuli-responsive materials, 4D printing has opened up new possibilities of creating 3D structures that can undergo programmed spatiotemporal changes, which can potentially lead to novel engineering systems with variable properties and functions. There are two groups of materials used in 4D printing. The first group is shape memory polymers (SMPs) that are mechanically deformed to other temporary shapes (shape programming) until heated above its glass transition temperature (T_g) when the "memorized" original printed shape is restored (shape recovery).[1–5] However, their stimuli-responsive morphing is only one-way in that mechanical processing is always required for shape programming. The second material group for 4D printing is stimuli-responsive hydrogels that show a substantial volume change by regulating water uptake.[6–9] Although the self-deformation of hydrogels is reversible depending on various environmental changes, hydrogels suffer from an extremely slow time-scale for shape change

[a] *Department of Mechanical and Aerospace Engineering, Rutgers University-New Brunswick, 98 Brett Road, Piscataway, NJ 08854, USA*
[b] *Department of Mechanical Engineering, Seoul National University, Seoul 08826, Republic of Korea. E-mail: howon.lee@snu.ac.kr*

due to a quadratic scaling law for the diffusive water molecule migration process. Furthermore, water-containing hydrogels are not suitable for applications where surrounding water is not available, which significantly restricts their practical applicability. Recently, liquid crystal elastomers (LCEs), combining polymeric elasticity with liquid crystalline anisotropy, have received growing attention as a new class of a 4D printing material that can overcome the limitations of SMPs and hydrogels. Since LCE's stimuli-responsive deformation is driven by re-orientation of their own molecular structure, they require neither external force nor aqueous environment for self-deformation. In addition, LCEs also possess other unique properties including high work density,[10–13] anisotropic mechanical/thermal/optical properties,[14–17] and high viscoelastic dissipation.[18–21] The extraordinary properties of LCEs, their chemistry and responsiveness to different physical cues, and how they are utilized to enable 4D printing have been extensively discussed in recent reviews.[22,23] We provide herein a succinct review on the physical principles underlying the key methods for LCE molecular programming and recent advances in LC alignment with various additive manufacturing processes to push the boundary of 4D printing. Various applications of additively manufactured LCEs are also highlighted. We believe that this mini-review offers a new perspective on LCE 4D printing in the context of LCE molecular programming with additive manufacturing.

2. Key strategies for liquid crystal alignment

LCEs are crosslinked polymers within which liquid crystal molecules are linked with elastomeric polymer chains. The unique properties of LCEs arise from their primary constituent molecules, liquid crystal (LC). LC molecules, also called mesogens, are an intermediate state of matter that can exhibit both liquid fluidity and solid crystalline order. Due to their elongated molecular shape, mesogens have intrinsic anisotropy which brings about flowability with long-range order, large birefringence, and the ability to align by external fields (mechanical, optical, electric, and magnetic).[24] Taking advantage of this property, LCE networks with an orientational order of mesogens can be synthesized. Upon external stimuli such as heat, the aligned mesogens undergo a transition between an ordered liquid crystalline state (nematic) and a disordered liquid state (isotropic) (Fig. 1). This order–disorder phase transition, called nematic-isotropic transition, takes place above a specific temperature (T_{NI}), resulting in macroscopic contraction and expansion of the LCE along and perpendicular to the alignment direction, respectively. When temperature is lowered, the elasticity of the polymeric network restores the order of the mesogens and, consequently, the LCE returns back to the undeformed shape. Since the first experimental demonstration,[25] the stimuli-responsive deformation of LCEs has opened an emerging research frontier in recent decades. The direction

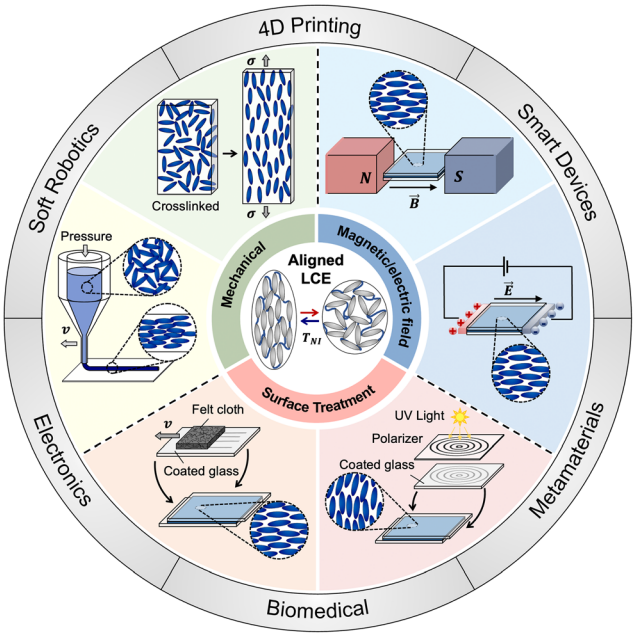

Fig. 1 Nematic-isotropic phase transition of mesogens in a liquid crystal elastomer (LCE) network gives rise responsive and reversible deformation. Various mesogen alignment strategies include mechanical alignment, magnetic/electric field alignment, and surface treatment.

and the magnitude of a reversible deformation of LCEs can be programmed through designing the orientational order mesogens in the LCE. To this end, an appropriate alignment treatment should be applied during fabrication process. The primary strategies for aligning mesogens in LCEs include mechanical extension, magnetic/electric field, and surface treatment (Fig. 1).

2.1. Mechanical alignment

Mechanical extension of a weakly crosslinked LCE network induces rotation of randomly oriented mesogens and thus aligns them along the stretching direction. Based on the pioneering work by Finkelmann, Yakacki *et al.* introduced a two-stage thiol-acrylate Michael addition and photopolymerization reaction.[26] In this method, a mixture of thiol-spacer, thiol-crosslinker, and acrylate-mesogen is prepared with an excess amount of acrylate groups inside. The first-stage thiol-acrylate Michael addition consumes all thiol groups and partial acrylate groups to form a flexible LCE oligomer in which mesogens are randomly distributed (called polydomain). Then, a uniaxial mechanical stretch is applied to align mesogens, followed by the second-stage photopolymerization to further crosslink the remaining acrylate groups in the stretched network, thereby permanently fixing the LC alignment in the crosslinked polymeric network (called monodomain) (Fig. 2a). At high temperatures above T_{NI}, the aligned mesogens become disordered, resulting in a temperature-responsive reversible deformation of the LCE. This method is simple and effective

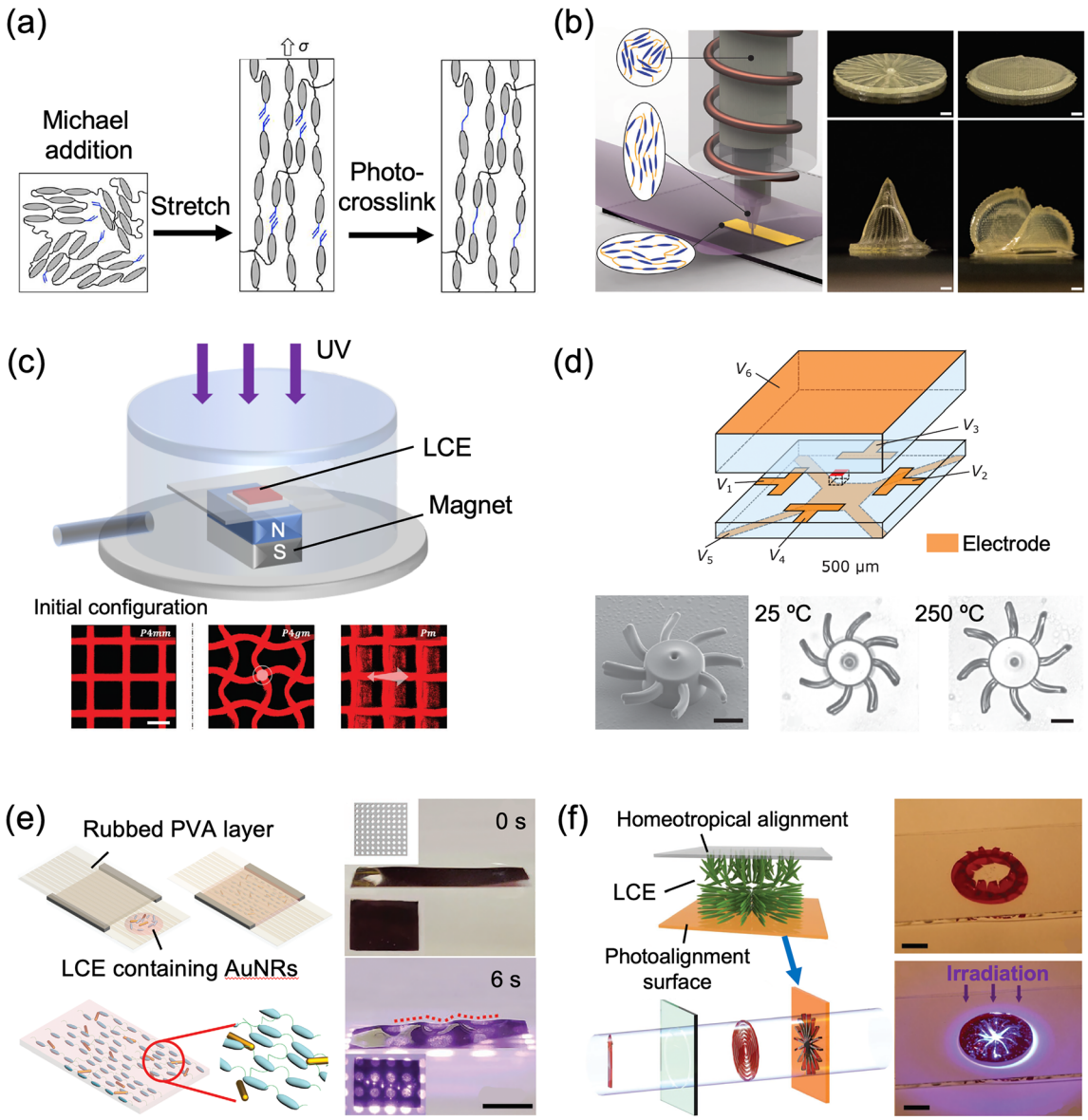

Fig. 2 LC molecule alignment methods. (a) Mechanical extension to align mesogens based on a two-stage thiol-acrylate Michael addition and photopolymerization reaction (reproduced from ref. 26 with permission from Royal Society Chemistry, copyright 2015). (b) LC alignment induced by shear stress developed in a viscous flow in direct ink writing (DIW); LCE discs of identical geometry printed with different printing paths morphing into different shapes upon heating (reproduced from ref. 31 with permission from John Wiley and Sons, copyright 2018). (c) Magnetic field alignment using a permanent magnets to spatially program mesogen orientations (reproduced from ref. 35 with permission from John Wiley and Sons, copyright 2021). (d) Electric field generated by three pairs of electrodes to three dimensionally align mesogens in a two photon polymerization printing (reproduced from ref. 39 under the terms of the Creative Commons CC BY license from John Wiley and Sons, copyright 2021). (e) LC alignment by uniaxially rubbed surfaces; LCE film capable of deforming in response to near-infrared (NIR) light (reproduced from ref. 47 with permission from John Wiley and Sons, copyright 2020). (f) Complex splayed LC alignment realized by a radially photoaligned surface and a homeotropically aligning surface (reproduced from ref. 54 with permission from John Wiley and Sons, copyright 2017).

to produce bulk LCEs with relatively large deformation and thus has been widely used to fabricate LCE-based devices. The transition temperature T_{NI} can also be tailored by controlling the ratio of elastomeric polymer chains to mesogens.[27] Due to the quadratic relation between dimension and time-scale by thermal conduction, decreasing the characteristic length-scale of the LCE (*e.g.* electrospun LCE fibers) can effectively speed up the response of LCEs.[11]

Using the same principle, more complex LCE deformation was achieved by multi-axial mechanical stretch. For example, LCE metamaterials showing a macroscopic biaxial actuation strain were fabricated by biaxially stretching laser-cut LCE followed by ultraviolet (UV) photopolymerization.[28,29] A variety of complicated LCE morphing has also been demonstrated by employing more complex mechanical programming such as twisting, stamping, and embossing.[30]

Although mechanical stretching has been shown to be an effective and simple method to fabricate various LCE structures, it is challenging to encode complex orientational orders of mesogens in LCEs, which is essential to diversify possible modes of LCE actuation.

LC molecules can also be aligned by shear stress developed in a viscous flow. Instead of applying mechanical extension to a lightly crosslinked LCE, this method exploits viscous shear flow of a nematic LCE ink with an appropriate rheological property. While flowing through a nozzle or a small gap, LC molecules are subjected to a strong shear stress in the extensional flow and thus aligned in the flow direction. This principle has been extensively used in direct ink writing (DIW) of LCEs.[31] The process-induced alignment of mesogens allows for complex LC orientation programming *via* designing printing path (Fig. 2b), as well as production LCEs in 3D geometries. However, the fact that mesogen alignment direction is always determined by the printing path is a shortcoming of this method. In a recent report, decoupling of geometric patterning and mesogen alignment was achieved by digital light processing (DLP)-based printing using a rotary tray that generates a shear-induced flow of an LCE resin in the projection area.[13]

2.2. Magnetic/electric field alignment

Anisotropic molecular structure of mesogens gives rise to highly anisotropic magnetic susceptibility of LC molecules. Therefore, their orientation can be manipulated in a non-contact manner by applying an external magnetic field. It should be noted that magnetic alignment requires a nematic state of mesogens in which molecular mobility and magnetic susceptibility anisotropy of LC molecules are high.[32] Also, a strong magnetic field on the order of hundreds millitesla is typically needed to magnetically align mesogens. Electromagnets such as Helmholtz coils can provide a uniform magnetic field with a controllable field strength, but as a required field strength increases, an experimental setup for electromagnets becomes increasingly bulky and expensive. Additional consideration should be given to thermal management, which further increases system cost. As such, permanent magnets such as neodymium (NdFeB) are used as an alternative source of a strong magnetic field.[33–37] For example, NdFeB magnets were used to fabricate LCE lattices with aligned mesogens, whose transformation was defined by programmed LC alignment (Fig. 2c).[35] However, temperature control should be typically performed together with magnetic alignment to switch between nematic and isotropic states, which caused challenges such as thermal expansion and long process time.[33,36] A recent study demonstrated magnetic alignment of mesogens without using repeated thermal cycles to reduce processing time, but it was still necessary to treat mesogens at high temperatures to keep them magnetically alignable in the nematic state.[37] While the same principle is applied for electric-field LC alignment, it is technically more challenging because an extremely high voltage is required.[38] A recent study proposed an electric-field LC alignment system with three pairs of electrodes to spatially control the orientation of the electric field in 3D (Fig. 2d).[39] In this way, LCE structures with various localized LC alignment were fabricated using multi-photon laser printing.

2.3. Surface treatment

Surface rubbing, micro-patterning, and photo-alignment exploit the surface anchoring effect of mesogens.[40,41] Surface anchoring is a complex phenomenon that involves the nature of LC material and coating material, which can be simply interpreted as an action that nematic LC molecules near a treated surface tend to be aligned due to the combination of an interaction with the specific coating material on such treated surface and geometrical factors.[42] In surface rubbing, a substrate (*e.g.* glass) is coated with a specific material (*e.g.* polyimide) and then mechanically rubbed to create microgrooves along the target nematic direction.[43–46] Mesogens in contact with the treated surface are oriented in this direction and crosslinked to form network by a subsequent polymerization reaction. For example, a photo-responsive LCE film with embedded gold nanorods (AuNRs) was fabricated in this method, which was able to deform in response to near-infrared (NIR) light as well as heat due to photo-thermal effect of AuNRs (Fig. 2e).[47] While rubbing on a surface is easy and readily accessible without expensive tools, alignment direction is limited to relatively simple patterns (*e.g.* uniaxial, biaxial, *etc.*).[47,48] More complex alignment patterns, and therefore diverse shape changes of LCEs, were achievable by photolithographically created micro-/nano surface patterns.[49–53] An approach was to employ a thin coating of a photo-responsive material whose radial pattern can be controlled by azimuthally polarized light. Spatially splayed LC alignment was realized when preparing such a surface and another homeotropically aligning surface (Fig. 2f).[54] Due to the weak surface anchoring effect, however, only mesogens that are very close to the treated surface can be effectively aligned. Therefore, the thickness of the fabricated LCE films is typically limited within about 100 μm. Limited use of surface treatment alignment in additive manufacturing has been reported in two photon polymerization direct laser writing (TPP-DLW) where fabrication length scale is usually small.

3. Additive manufacturing of LCEs

Additive manufacturing (AM) has rapidly expanded its material selection in the past decade. Employing various responsive materials, AM can now precisely manufacture complex objects that can transform over time in response to external stimuli. LCEs have received growing attention as an

emerging AM material due to their programmable and reversible deformation. Extensive efforts have been recently made in order to achieve prescribed molecular order of mesogens in 3D printed LCEs. Due to different material processing strategies of AM, different AM approaches employ a more advantageous mesogen alignment strategy. For example, viscous shear can be readily utilized in DIW using a material extrusion nozzle, while a magnetic/electric field is better suited for DLP where no mechanical obstructions are permitted along the optical projection path. Surface treatment is a more viable method in two-photon polymerization (TPP) because overall size of a printed object is within the range of the surface effect. Here we provide a brief review on various strategies for AM of LCEs with spatially programmed mesogen alignment.

3.1. Direct ink writing

DIW is the most widely used AM method for LCEs (Fig. 3a). Mesogens are aligned by the shear flow induced while viscous ink is extruded through a nozzle. Consequently, nematic director orientation in the printed LCE is aligned along the nozzle path. Therefore, spatial arrangement of LC orientation in the printed LCE is determined by designing printing nozzle trajectory. For example, geometrically identical LCE discs transformed into different shapes, a cone and a saddle, when the printing path was along the radial and the circumferential directions, respectively (Fig. 2b).[31] Furthermore, DIW printing path can be used to create intentional anisotropy in the printed LCE, resulting in enhanced impact absorption and tailorable buckling

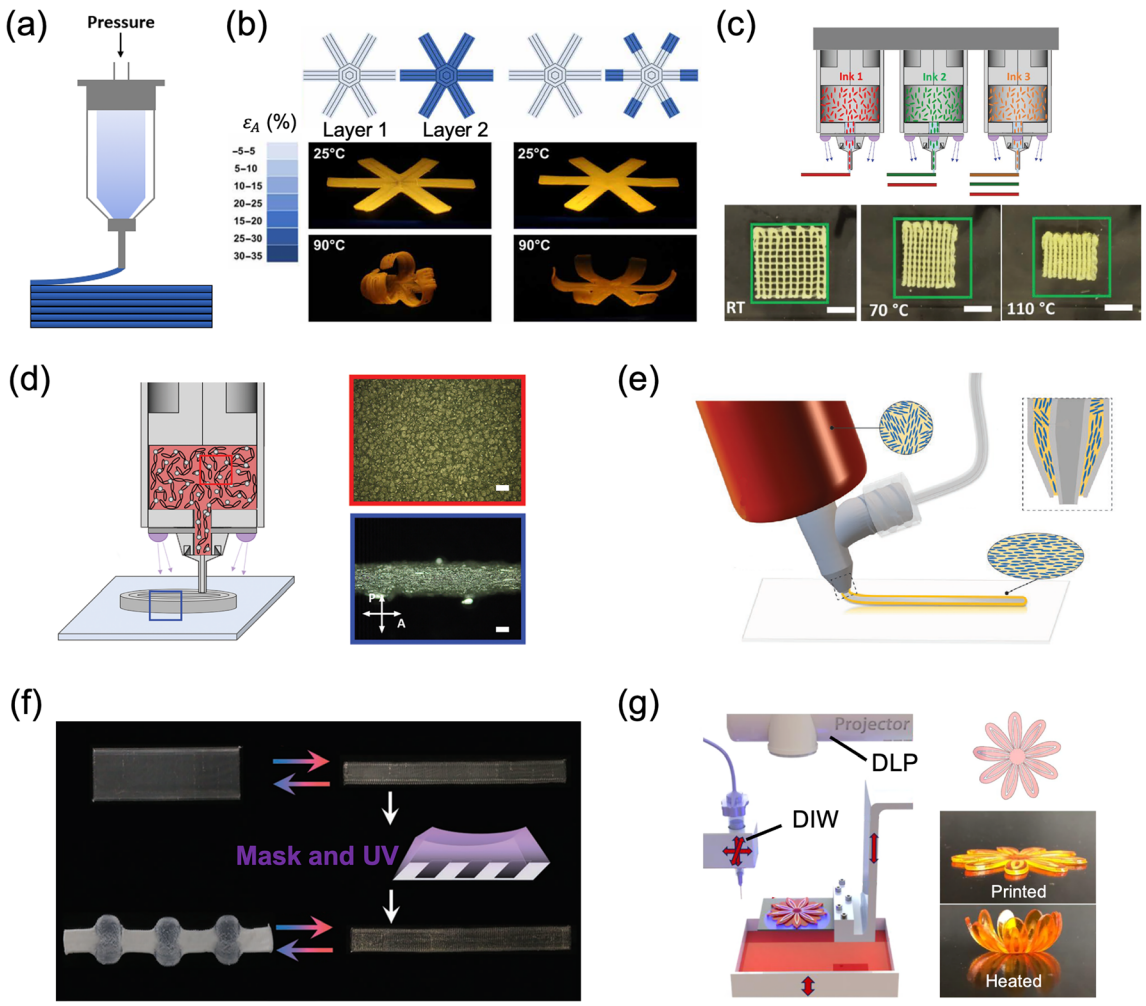

Fig. 3 Direct ink writing (DIW) of LCEs. (a) Schematic of DIW process. (b) DIW-printed bilayer structures showing different temperature responsive deformations depending on printing process parameters (reproduced from ref. 55 with permission from AAAS, copyright 2020). (c) LCEs with tunable nematic-isotropic transition temperatures (T_{NI}) printed through DIW; sequential deformation of a log pile structure fabricated by different LCE materials (reproduced from ref. 60 with permission from John Wiley and Sons, copyright 2018). (d) DIW printing of an electro-actuated structure using LCE ink with dispersed liquid metal (reproduced from ref. 67 with permission from American Chemical Society, copyright 2021). (e) Coaxial extrusion DIW with a liquid metal core surrounded by a LCE shell (reproduced from ref. 12 with permission from John Wiley and Sons, copyright 2021). (f) DIW printing of LCE structures with light-triggerable dynamic bonds for temporary shape fixing and shape recovery (reproduced from ref. 68 with permission from John Wiley and Sons, copyright 2019). (g) Hybrid multi-material 3D printing system with integrated DIW and digital light processing (DLP) printing (reproduced from ref. 70 with permission from Elsevier, copyright 2021).

behavior.[20] It has also been shown that the responsive behavior of the printed LCE structure is determined by various process parameters including extrusion flow rate, nozzle size, nozzle speed, stand-off distance, and rheological property of the extruded ink (Fig. 3b).[17,55–57] A coaxial extrusion needle was also used to achieve LC alignment in DIW.[58] The sheath flow around the LCE ink caused the mesogens to align along the extrusion direction.

High flexibility in printing material of DIW permits exploration of a wide range of LCE material variants for tunable properties and diverse functionalities. For enhanced printability and facile actuation without the need for excessive heating, an ink formulation for an LCE with low T_{NI} of approximately 42 °C was proposed.[59] LCE inks with different T_{NI} were also printed using multi-material DIW for sequential deformation of the printed LCE structures (Fig. 3c).[60–62] Multimodal shape changes were also demonstrated using multi-material DIW with LCE inks that are responsive to heat, UV light, or humidity.[63–66] Electrically conductive LCE structures were achieved by adding liquid metal (*e.g.*, eutectic gallium indium, eGaIn) in a LCE ink as dispersed droplets (Fig. 3d)[67] or by co-extruding eGaIn with a LCE ink through a coaxial nozzle (Fig. 3e).[12] The liquid metal-LCE composites served as an integrated resistive heater for direct heating for the actuation of the printed LCE structures, eliminating the need for environmental heating or additional heating circuit. SMP-like behaviors such as temporary shape fixing and on-demand shape recovery were demonstrated in LCEs by incorporating dynamic covalent bonding in the crosslinked network (Fig. 3f).[68,69]

DIW process has inherent shortcomings such as limited range of printable geometries, slow throughput due to serial nature of the process, and frequent clogging of a nozzle for highly viscous inks. LCE printing with DIW inherits these challenges. For more diverse LCE shapes, two-step polymerization method was employed in DIW printing of LCEs.[30] After a simple geometry was first printed with an LCE in a catalyst bath for partial crosslinking, it was

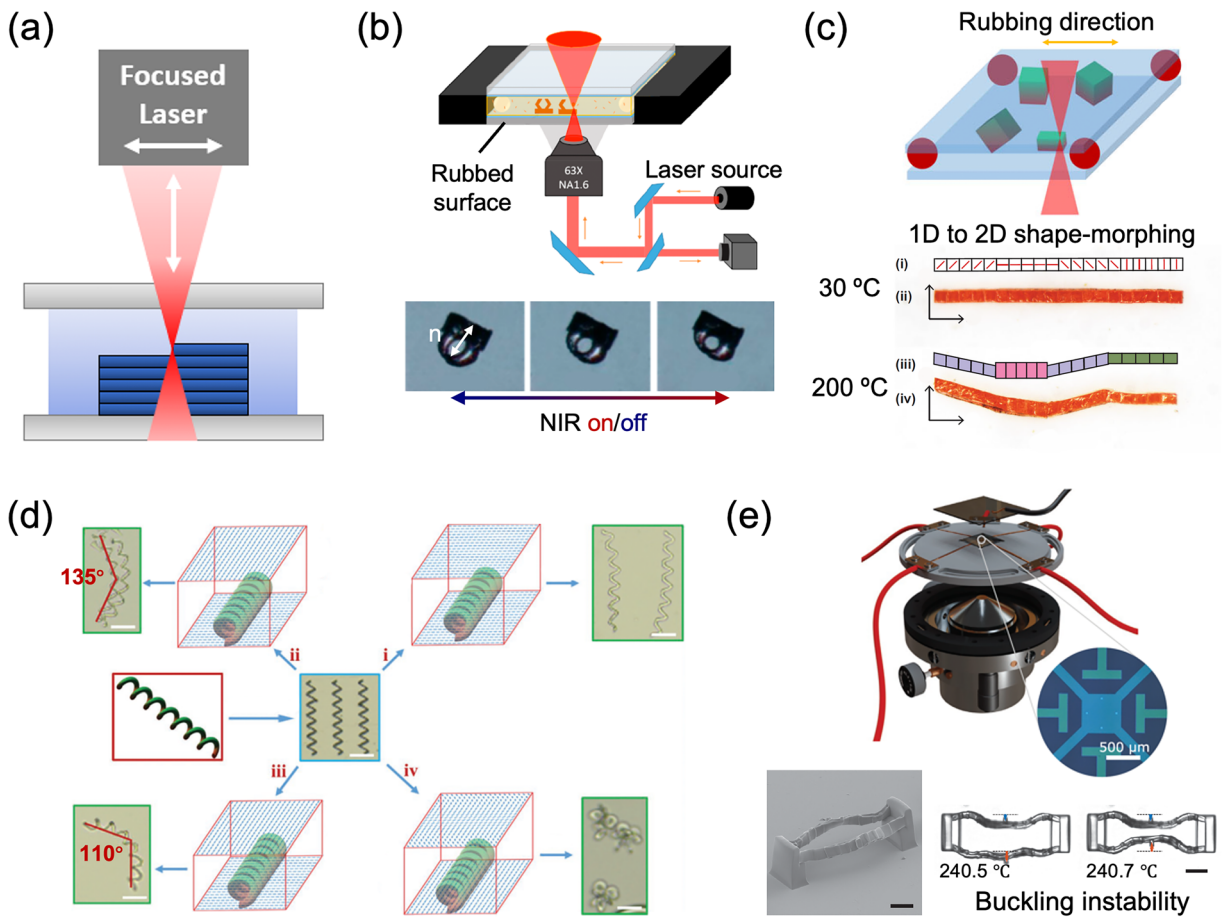

Fig. 4 Two photon polymerization (TPP) of LCEs. (a) Schematic of TPP process. (b) TPP printing of light-responsive LCE structures in which LCs are aligned by surface treatment (adapted from ref. 74 with permission from American Chemical Society, copyright 2019). (c) Complex shape-morphing of an assembly of TPP-printed cubic LCE voxels with a predefined mesogen director orientation (reproduced from ref. 76 under the terms of the Creative Commons CC BY license from Springer Nature, copyright 2021). (d) Different shape-morphing of TPP-printed LCEs programmed by various topological surface treatment (reproduced from ref. 78 under the terms of the Creative Commons CC BY license from John Wiley and Sons, copyright 2020). (e) TPP printing of LCEs with complex electric-field mesogen alignment (reproduced from ref. 39 under the terms of the Creative Commons CC BY license from John Wiley and Sons, copyright 2021).

mechanically deformed to a desired complex shape, by which mesogen alignment is programmed. The subsequent polymerization with UV exposure was applied to fix the deformed shape. Also, to improve the process speed, a hybrid printing system was proposed where LCE ink was printed on top of a 3D structure printed with DLP (Fig. 3g).[70] A highly viscous LCE ink was also successfully printed with DIW printing at an elevated temperature above T_{NI}.[71]

3.2. Two photon polymerization

Two-photon polymerization (TPP) utilizes the two-photon absorption to polymerize a photo-curable resin at the focal spot of a femtosecond NIR laser (Fig. 4a). Therefore, a complex 3D structure with dimensions from submicron to a few hundred μm can be achieved. Considering this length scale, LC alignment with surface treatment fits well with TPP process because the effect of surface treatment is still present within about 100 μm. The simplest approach is to infiltrate a photocurable LCE precursor solution in a small gap (*e.g.*, 50 μm) between two glass slides coated with uniaxially rubbed polyimide surfaces. The result showed that a homogeneous mesogen orientation was achieved in 3D LCE structures fabricated using TPP inside this confined space.[72,73] A similar method was applied to an LCE precursor solution containing various photothermal nanofillers such as AuNRs to achieve complex light-responsive LCE micro-actuators (Fig. 4b).[74] Also studied was the printability of LCEs containing various photothermal materials with TPP, including multiwalled carbon nanotubes, graphene oxide, and AuNRs.[75]

Although surface treatment can generate relatively simple alignment only, assembly of TPP printed cubic LCE voxels with a predefined director orientation was demonstrated to attain 3D structures with arbitrary LC-director fields displaying a broad range of morphing modes (Fig. 4c).[76] For more diverse alignment patterns, TPP itself was used to first create topological gratings on a surface, which in turn was used as a printing substrate to align mesogens while printing 3D LCEs with TPP (Fig. 4d).[77,78] Optically transparent electrodes were used to generate arbitrary electric field vectors in 3D that enabled 3D LC alignment in TPP printed LCE structures (Fig. 4e).[39]

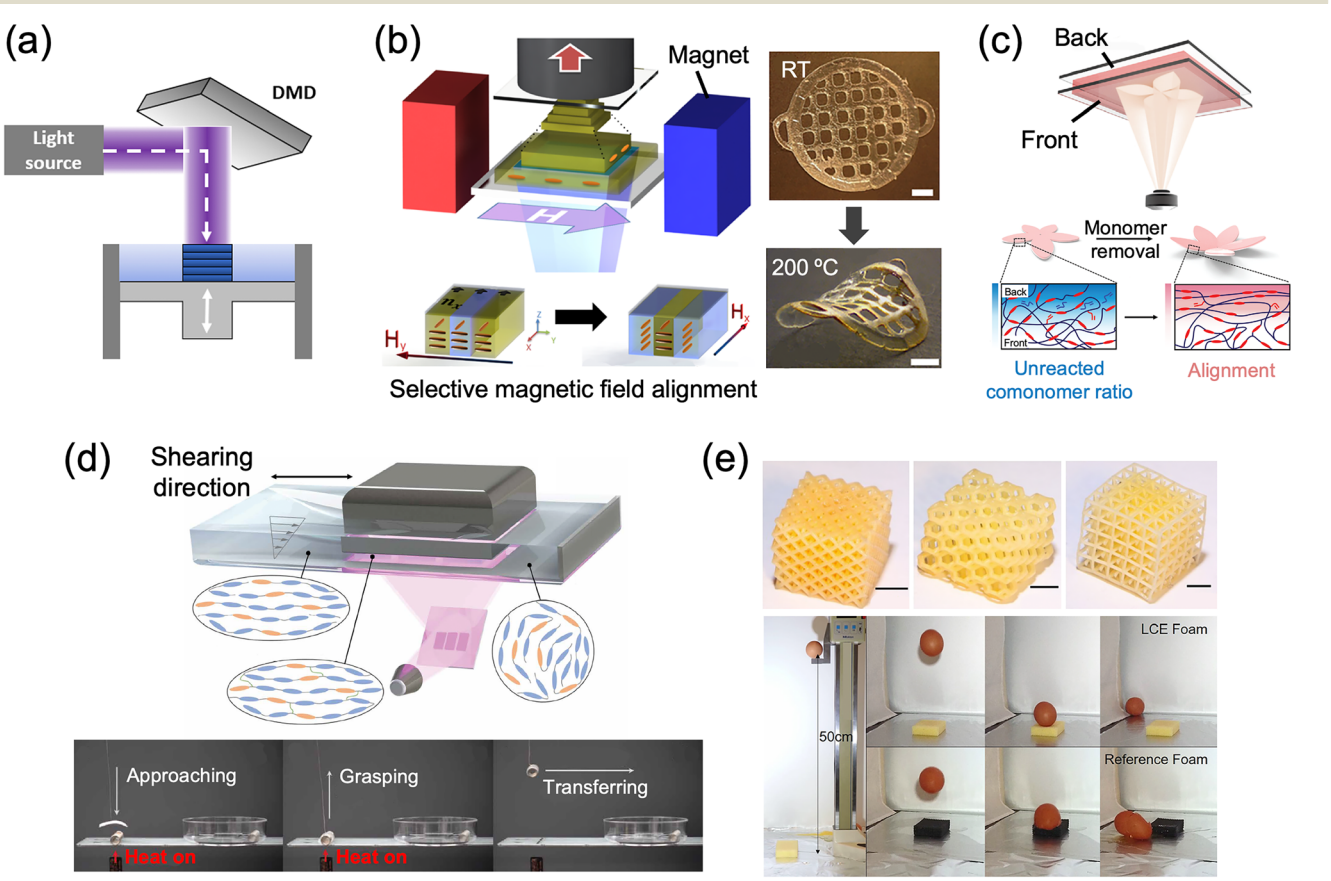

Fig. 5 Digital light processing (DLP) of LCEs. (a) Schematic of DLP process. (b) Magnetic-field-assisted DLP printing for programmable LC alignment (reproduced from ref. 37 with permission from American Chemical Society, copyright 2019). (c) DLP-printed LCEs with an in-depth LC alignment gradient (reproduced from ref. 80 with permission from John Wiley and Sons, copyright 2021). (d) DLP printing of LCEs with shear-flow-induced LC alignment. (reproduced from ref. 13 with permission from AAAS, copyright 2021). (e) LCE microlattices with high energy absorption (reproduced from ref. 19 with permission from American Chemical Society, copyright 2021).

3.3. Digital light processing-based AM

DLP-based AM is a stereolithography technique using a digital micro-mirror device (DMD) as a dynamically reconfigurable digital photomask to solidify a liquid resin into a 3D object *via* UV photopolymerization (Fig. 5a). The fact that no mechanical obstructions are allowed along the optical projection path in a DLP printing system presents a particular challenge for incorporating a mesogen alignment mechanism. Among a few reported efforts, mesogen alignment using a magnetic field during DLP process showed some promise. Exploiting the diamagnetism of mesogenic LC molecules,[32] a reorientable permanent magnet pair with a magnetic strength of 0.3 T was employed to align mesogens. Projection of a patterned UV light on a selective area was followed to produce LCE with the desired mesogen alignment (Fig. 5b).[37] However, the entire process has to be performed at a high temperature in order to keep the mesogens in the nematic state, in which mesogens are orientable with a magnetic field.[79] Also, because of the requirement for clearance in the optical path, only in-plane alignment was possible. Alignment in out-of-plane direction was achieved by harnessing the intrinsic light attenuation of DLP printing in the depth direction.[80] As a result, a crosslinking-density gradient in LCE was created along the thickness, and subsequent evaporation of unreacted monomers not only induced a slight bending, but also created a gradient of LC alignment along the thickness (Fig. 5c). In-plane mesogen orientations, however, cannot be controlled by this method. A DLP system employing viscous shear to align mesogens was also demonstrated.[13] A rotating resin tray was integrated in a DLP system to a shear flow through the gap between the resin tray and the print head. Mesogens were then aligned along the flow direction and polymerized by UV projection (Fig. 5d). Limitations of this method are the monotonous and in-plain alignment direction and shear gradient created in the depth direction.

Regardless of the control of LC orientation, other unique properties of LCEs have also been explored through DLP 3D printing. It has been reported that the viscoelastic relaxation and the mechanically induced phase transition of the LCE network both contributed to extraordinary energy dissipation of 3D LCE microlattices (Fig. 5e).[18,19] A multi-material DLP system with multiple resin vats was used to fabricate smart optical devices with LCE displaying variable optical transparency around T_{NI}.[81]

4. Applications of additively manufactured LCEs

With unique characteristics including stimuli-responsive deformation, anisotropic properties, and soft elasticity, LCEs offer great promise in many fields such as soft robotics,[82,83] electronics,[84,85] and smart devices.[86,87] However, relatively plane geometries (*e.g.* film, strip, plate) and simple deformation modes (*e.g.* uniaxial contraction) of LCEs significantly limit their further applications. With the recent progress in additive manufacturing technologies, LCEs have been rapidly expanding their reach across a broad spectrum of application sectors.

LCEs have been proven to offer tremendous potential for soft robots and artificial muscles due to their substantial actuation strain and high work density, which are comparable to those of mammalian skeletal muscles.[10] Numerous LCE applications constructed using the DIW approach have been reported because DIW provides the easiest and most convenient mesogen alignment method for 3D printing. Recently, long LCE fibers were obtained by harnessing DIW-based extrusion onto a rotating mandrel.[88] These fibers were used to create a smart textile with breathable pores that can open and close in response to the environment and wearer's body temperature (Fig. 6a). Utilizing multi-material DIW printing, actuatable LCE can be easily incorporated with other structural polymers. A passive polymer structure with LCE joints was printed together to create an untethered self-propelling robot.[61] It was printed as a 2D structure, which then morphed into a 3D roller and rolled forward when placed on a heated surface (Fig. 6b). DIW-printing was also used to create a soft robotic gripper and a printed hand with elastomer, conductive ink, and LCE.[59] The layer-wise integration of the passive elastomer and the active LCE enabled the unidirectional bending of each gripper hinge (Fig. 6c). LCE fibers with a liquid metal core were produced using a coaxial nozzle in the DIW system to fabricate an electroactive artificial arm for a robotic system[12,58] (Fig. 6d). Besides DIW, TPP with the surface treatment alignment approach was employed to develop a micro-scale light-driven locomotor (~50 μm).[89] In response to periodic laser irradiation, the micro-walker repeatedly altered the volume of the body to achieve forward motion on a specific substrate (Fig. 6e). With DLP, a robotic arm having two parts that can move depending on light and temperature, respectively, was created.[37]

Responsive to temperature or light, LCEs can be used for remote control of printed structures. LCEs were used to develop a smart switch to allow remote control of an electric circuit's "on/off" state.[67] A DIW ink with dispersed liquid metal droplets displayed electric conductivity and NIR-responsive deformation, which was exploited to demonstrate a light-driven electric switch (Fig. 6f). Braille-like display was also demonstrated with a DIW-printed LCE showing a photo-switchable deformation (Fig. 4g).[69] LCE with a tailored T_{NI} was developed and employed to demonstrate a sequential actuation of the DIW-printed structure.[62] Furthermore, kirigami metastructure was printed using TPP directly on a uniaxially aligned LCE substrate.[90] Taking advantage of an aligned LCE's expansion in the direction perpendicular to the mesogen alignment, the stretching of a kirigami metastructure was accomplished by remote heating of the LCE substrate.

Novel applications have also been proposed using the unique optical properties of LCEs. A study reported a chiral

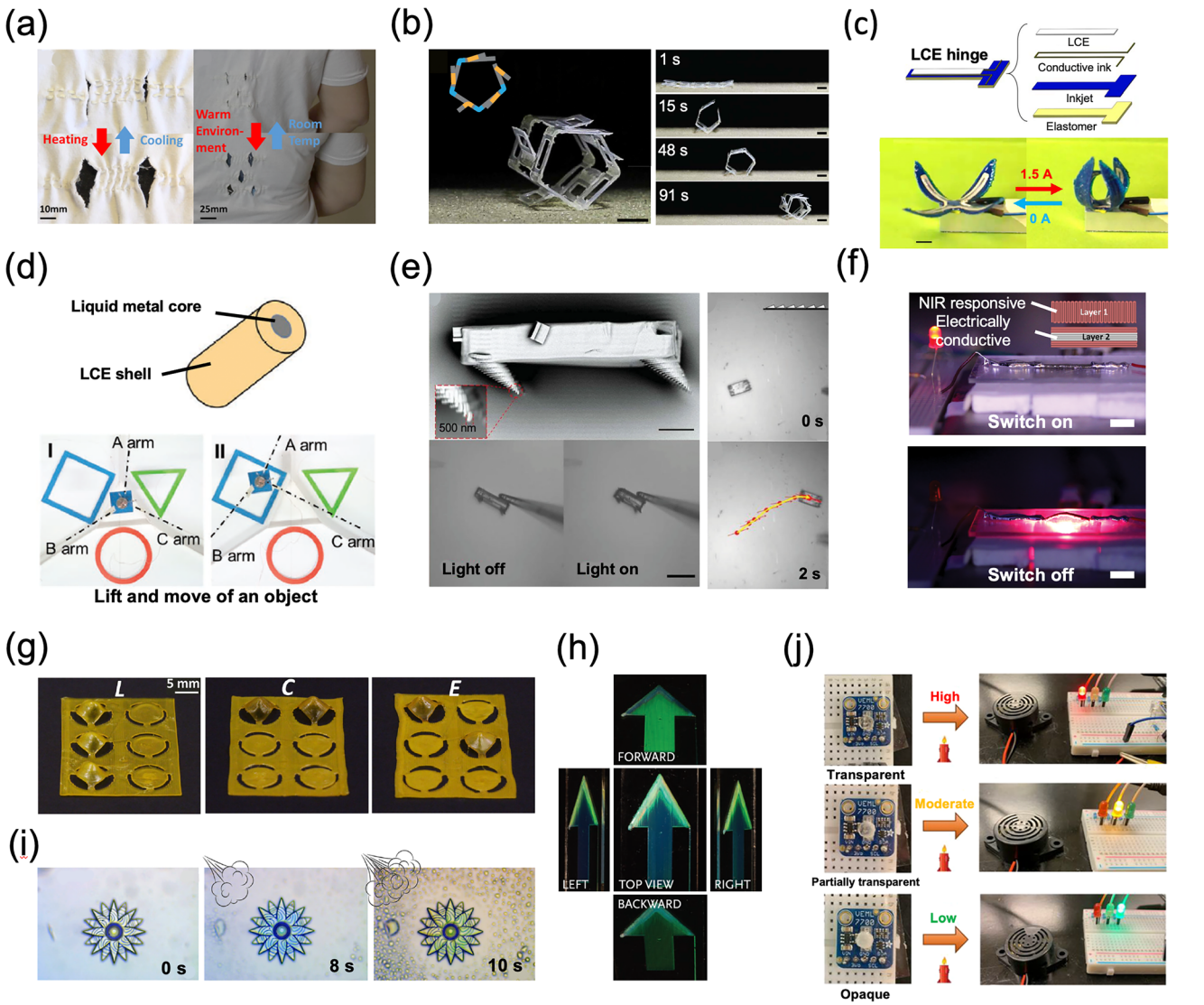

Fig. 6 Applications of additively manufactured LCEs. (a) Smart LCE textile with breathable pores for body temperature regulation (reproduced from ref. 88 with permission from American Chemical Society, copyright 2019). (b) Untethered self-propelling robot with LCE hinges (reproduced from ref. 61 with permission from American Association for the Advancement of Science, copyright 2019). (c) Soft LCE gripper composed of passive elastomer and active LCE and driven by electrothermal input (reproduced from ref. 59 with permission from IOP Publishing, copyright 2018). (d) Robotic arm system consisting of three electro-activated LCE arms (reproduced from ref. 58 with permission from John Wiley and Sons, copyright 2021). (e) Light-actuated micro-walker printed by TPP (reproduced from ref. 89 with permission from John Wiley and Sons, copyright 2015). (f) LCE switch operated with NIR light (reproduced from ref. 67 with permission from American Chemical Society, copyright 2021). (g) DIW-printed Braille-like actuator displaying letters (reproduced from ref. 69 with permission from John Wiley and Sons, copyright 2021). (h) DIW-printed cholesteric LCE structure showing different surface color distributions depending on perspective (reproduced from ref. 57 with permission from John Wiley and Sons, copyright 2021). (i) TPP-printed cholesteric LCE micro-flower displaying a color change upon exposure to a high humidity (reproduced from ref. 91 under the terms of the CC-BY-NC-ND 4.0 license from American Chemical Society, copyright 2020). (j) Temperature sensor utilizing temperature-dependent transparency of LCE (reproduced from ref. 81 with permission from American Chemical Society, copyright 2022).

nematic LCE ink that self-assembled into chiral photonic structures with cholesteric LC alignment.[57] With a controllable DIW printing speed of 10 mm s^{-1}, the normal helical director in the deposited filaments was angled so that these filaments reflected light independent of circular polarization, thereby producing a structural color exhibiting a considerable perspective dependency (Fig. 6h). Moreover, color change of cholesteric LCE structures was also achieved by volume expansion of the helix director in a humid environment. Similarly, a photonic micro-flower with a cholesteric LC alignment was manufactured using TPP, whose color shifted from transparent to blue to green as the environmental humidity changed (Fig. 6i).[91] LCEs are opaque in the nematic polydomain state and become transparent when it is heated to the isotropic regime. This optical behavior of LCEs was leveraged to develop a temperature

sensor, where optical transmission of the LCE was monitored to detect temperature rise above a safety threshold (Fig. 6j).[81]

5. Conclusions and outlook

LCEs have distinctive properties including anisotropic mechanical/thermal/optical properties, high viscoelastic dissipation, and high work density during stimuli-responsive deformation, just to name a few. The great potential of LCEs can be further enhanced and eventually lead to more practical applications when geometrical diversity and dimensional accuracy are combined with unique characteristics of LCEs *via* additive manufacturing. To this end, it is essential to implement a mesogen alignment method in a suitable AM process to program the spatial arrangement of mesogen orientation. To date, several key alignment methods have been proposed, including mechanical stretch, viscous shear, magnetic/electric-field, and surface treatment. Each of these approaches has its own strength and weakness. For example, mechanical stretch is straightforward to perform, but always necessitates extensive deformation of the crosslinked LCE for mesogen orientation programming, which significantly restricts the range of accessible geometry of the final LCE devices. Although viscous shear is a method frequently employed in DIW and provides precise geometric control over mesogen alignment in the printed LCEs, the alignment direction is strongly tied to the extrusion nozzle path. Magnetic/electric-field alignment is a non-contact alignment approach that allows for the programming of mesogens in any arbitrary directions, but the necessary instrumentation to produce sufficient field strength poses technical difficulties. Surface treatment is simple and easy, but the alignment effect is strictly limited to the immediate vicinity of the treated surface. Since all of the aforementioned strategies rely on different physical principles, a suitable alignment method should be implemented based on the AM process in order to achieve prescribed molecular orientation of mesogens in 3D printed LCEs. As briefly reviewed in this article, various approaches to accomplish molecular programming of mesogens during 3D printing LCEs have been reported.

Despite the remarkable advances in 4D printing with LCEs in recent years, there are still outstanding challenges that need to be addressed. First, printable LCE inks rely heavily on the two-step "click" addition chemistry (or so-called Michael addition reaction).[59,60,92] This often causes the LCE ink's viscosity to significantly rise. While increasing the printing temperature may reduce the viscosity during printing,[31,55,61] it may also cause the polymers in the ink to degrade. Maintaining a high temperature environment could potentially be costly, depending on the printing method.[37,80] Using organic solvents such as toluene or dichloromethane is probably the most popular method to lower the viscosity of LCE inks and keep them in a nematic state.[13,18] However, removing volatile solvent from the printed LCE inevitably causes considerable volumetric shrinkage, resulting in a final geometry and dimension of the LCE very different from the original design. More studies on thermomechanical/rheological properties of printable LCE inks would accelerate the advance of 4D printing with LCEs. Second, current LC alignment strategies in additive manufacturing are too simple to fully realize the promise of LCEs. LC alignment is strongly coupled with the nozzle path in DIW.[17] In the surface treatment method for TPP, it is strictly constrained to in-plane directions.[76] Shear flow used in DLP can only induce a unidirectional LC alignment.[13] Although magnetic/electric fields can increase the degrees of freedom of LC alignment, they often necessitate complex and expensive instrumentation.[37,39] Incorporation of a simple, affordable, and versatile LC alignment mechanism in an additive manufacturing platform would significantly expand the range of possible shape transformation modes of LCEs. Third, activation for LCE shape transformation mostly relies on applying a homogeneous field such as a uniform temperature, using a hot plate or temperature oven. Local or partial heating of LCEs through resistive heating has been demonstrated by embedding a conductive trace[59] or liquid metal inclusions,[12,67] but at the cost of increased density and reduced flexibility. Using azobenzene-based LCEs[63,93] or LCEs containing dispersed or coated photo-thermal agents[47,94] could be an alternative for local control of LCE shape change, but it only causes deformation at the surface of the LCE due to a limited light penetration depth. Another roadblock to reducing LCE transformation cycle time is that deactivation of LCEs is typically done by natural cooling.[95] Although there are still remaining challenges and technical obstacles, additive manufacturing of LCEs is specifically gaining ground as next generation 4D printing because of the advantages of LCEs over SMPs and hydrogels. We believe that the recent advances in additive manufacturing and materials development of LCEs will stimulate further exploration of new mesogen alignment techniques, innovative approaches to achieve molecular orders during AM process, and a broad spectrum of LCE applications.

Conflicts of interest

The authors declare no competing financial interests.

Acknowledgements

This work was supported by the National Research Foundation of Korea (NRF) grant funded by the Korea government (MSIT) (No. 1711154190) through the Institute of Advanced Machines and Design at the Seoul National University (SNU) and SNU Creative-Pioneering Researchers Program through the Institute of Engineering Research at SNU. Y. W. and H. L. gratefully acknowledge the partial financial support from Rutgers University Busch Biomedical Grant Program.

References

1 Q. Ge, A. H. Sakhaei, H. Lee, C. K. Dunn, N. X. Fang and M. L. Dunn, Multimaterial 4D Printing with Tailorable Shape Memory Polymers, *Sci. Rep.*, 2016, **6**, 31110, DOI: **10.1038/srep31110**.

2 D. Raviv, W. Zhao, C. McKnelly, A. Papadopoulou, A. Kadambi, B. Shi, S. Hirsch, D. Dikovsky, M. Zyracki, C. Olguin, R. Raskar and S. Tibbits, Active Printed Materials for Complex Self-Evolving Deformations, *Sci. Rep.*, 2014, **4**, 7422, DOI: **10.1038/srep07422**.

3 Q. Ge, H. J. Qi and M. L. Dunn, Active materials by four-dimension printing, *Appl. Phys. Lett.*, 2013, **103**, 131901, DOI: **10.1063/1.4819837**.

4 C. Yang, M. Boorugu, A. Dopp, J. Ren, R. Martin, D. Han, W. Choi and H. Lee, 4D printing reconfigurable, deployable and mechanically tunable metamaterials, *Mater. Horiz.*, 2019, **6**, 1244–1250, DOI: **10.1039/C9MH00302A**.

5 C. Yang, J. Luo, M. Polunas, N. Bosnjak, S. D. Chueng, M. Chadwick, H. E. Sabaawy, S. A. Chester, K. Lee and H. Lee, 4D-Printed Transformable Tube Array for High-Throughput 3D Cell Culture and Histology, *Adv. Mater.*, 2020, **32**, 2004285, DOI: **10.1002/adma.202004285**.

6 A. Sydney Gladman, E. A. Matsumoto, R. G. Nuzzo, L. Mahadevan and J. A. Lewis, Biomimetic 4D printing, *Nat. Mater.*, 2016, **15**, 413–418, DOI: **10.1038/nmat4544**.

7 D. Han, Z. Lu, S. A. Chester and H. Lee, Micro 3D Printing of a Temperature-Responsive Hydrogel Using Projection Micro-Stereolithography, *Sci. Rep.*, 2018, **8**, 1963, DOI: **10.1038/s41598-018-20385-2**.

8 D. Han, C. Farino, C. Yang, T. Scott, D. Browe, W. Choi, J. W. Freeman and H. Lee, Soft Robotic Manipulation and Locomotion with a 3D Printed Electroactive Hydrogel, *ACS Appl. Mater. Interfaces*, 2018, **10**, 17512–17518, DOI: **10.1021/acsami.8b04250**.

9 D. Han, Y. Wang, C. Yang and H. Lee, Multimaterial Printing for Cephalopod-Inspired Light-Responsive Artificial Chromatophores, *ACS Appl. Mater. Interfaces*, 2021, **13**, 12735–12745, DOI: **10.1021/acsami.0c17623**.

10 Q. He, Z. Wang, Z. Song and S. Cai, Bioinspired Design of Vascular Artificial Muscle, *Adv. Mater. Technol.*, 2019, **4**, 1800244, DOI: **10.1002/admt.201800244**.

11 Q. He, Z. Wang, Y. Wang, Z. Wang, C. Li, R. Annapooranan, J. Zeng, R. Chen and S. Cai, Electrospun liquid crystal elastomer microfiber actuator, *Sci. Robot.*, 2021, **6**, eabi9704, DOI: **10.1126/scirobotics.abi9704**.

12 A. Kotikian, J. M. Morales, A. Lu, J. Mueller, Z. S. Davidson, J. W. Boley and J. A. Lewis, Innervated, Self-Sensing Liquid Crystal Elastomer Actuators with Closed Loop Control, *Adv. Mater.*, 2021, **33**, 2101814, DOI: **10.1002/adma.202101814**.

13 S. Li, H. Bai, Z. Liu, X. Zhang, C. Huang, L. W. Wiesner, M. Silberstein and R. F. Shepherd, Digital light processing of liquid crystal elastomers for self-sensing artificial muscles, *Sci. Adv.*, 2021, **7**, eabg3677, DOI: **10.1126/sciadv.abg3677**.

14 J. Shin, M. Kang, T. Tsai, C. Leal, P. V. Braun and D. G. Cahill, Thermally Functional Liquid Crystal Networks by Magnetic Field Driven Molecular Orientation, *ACS Macro Lett.*, 2016, 6.

15 D. R. Merkel, N. A. Traugutt, R. Visvanathan, C. M. Yakacki and C. P. Frick, Thermomechanical properties of monodomain nematic main-chain liquid crystal elastomers, *Soft Matter*, 2018, **14**, 6024–6036, DOI: **10.1039/C8SM01178H**.

16 C. Luo, C. Chung, C. M. Yakacki, K. Long and K. Yu, Real-Time Alignment and Reorientation of Polymer Chains in Liquid Crystal Elastomers, *ACS Appl. Mater. Interfaces*, 2022, **14**(1), 1961–1972, DOI: **10.1021/acsami.1c20082**.

17 Z. Wang, N. Boechler and S. Cai, Anisotropic mechanical behavior of 3D printed liquid crystal elastomer, *Addit. Manuf.*, 2022, **52**, 102678, DOI: **10.1016/j.addma.2022.102678**.

18 N. A. Traugutt, D. Mistry, C. Luo, K. Yu, Q. Ge and C. M. Yakacki, Liquid-Crystal-Elastomer-Based Dissipative Structures by Digital Light Processing 3D Printing, *Adv. Mater.*, 2020, **32**, 2000797, DOI: **10.1002/adma.202000797**.

19 C. Luo, C. Chung, N. A. Traugutt, C. M. Yakacki, K. N. Long and K. Yu, 3D Printing of Liquid Crystal Elastomer Foams for Enhanced Energy Dissipation Under Mechanical Insult, *ACS Appl. Mater. Interfaces*, 2021, **13**, 12698–12708, DOI: **10.1021/acsami.0c17538**.

20 D. Mistry, N. A. Traugutt, B. Sanborn, R. H. Volpe, L. S. Chatham, R. Zhou, B. Song, K. Yu, K. N. Long and C. M. Yakacki, Soft elasticity optimises dissipation in 3D-printed liquid crystal elastomers, *Nat. Commun.*, 2021, **12**, 6677, DOI: **10.1038/s41467-021-27013-0**.

21 M. O. Saed, W. Elmadih, A. Terentjev, D. Chronopoulos, D. Williamson and E. M. Terentjev, Impact damping and vibration attenuation in nematic liquid crystal elastomers, *Nat. Commun.*, 2021, **12**, 6676, DOI: **10.1038/s41467-021-27012-1**.

22 M. del Pozo, J. A. H. P. Sol, A. P. H. J. Schenning and M. G. Debije, 4D Printing of Liquid Crystals: What's Right for Me?, *Adv. Mater.*, 2021, 2104390, DOI: **10.1002/adma.202104390**.

23 Z. Guan, L. Wang and J. Bae, Advances in 4D printing of liquid crystalline elastomers: materials, techniques, and applications, *Mater. Horiz.*, 2022, **9**, 1825–1849, DOI: **10.1039/D2MH00232A**.

24 D. Demus, J. W. Goodby, G. W. Gray, H.-W. Spiess and V. Vill, *Handbook of liquid crystals, volume 2A: low molecular weight liquid crystals I: calamitic liquid crystals*, John Wiley & Sons, 2011.

25 J. Küpfer and H. Finkelmann, Nematic liquid single crystal elastomers, *Makromol. Chem., Rapid Commun.*, 1991, **12**, 717–726.

26 C. Yakacki, M. Saed, D. Nair, T. Gong, S. Reed and C. Bowman, Tailorable and programmable liquid-crystalline elastomers using a two-stage thiol–acrylate reaction, *RSC Adv.*, 2015, **5**, 18997–19001.

27 R. K. Shaha, A. H. Torbati and C. P. Frick, Body-temperature shape-shifting liquid crystal elastomers, *J. Appl. Polym. Sci.*, 2021, **138**, 50136, DOI: **10.1002/app.50136**.

28 J. Wu, S. Yao, H. Zhang, W. Man, Z. Bai, F. Zhang, X. Wang, D. Fang and Y. Zhang, Liquid Crystal Elastomer

Metamaterials with Giant Biaxial Thermal Shrinkage for Enhancing Skin Regeneration, *Adv. Mater.*, 2021, **33**, 2106175, DOI: **10.1002/adma.202106175**.

29 Y. Li, H. Yu, K. Yu, X. Guo and X. Wang, Reconfigurable Three-Dimensional Mesotructures of Spatially Programmed Liquid Crystal Elastomers and Their Ferromagnetic Composites, *Adv. Funct. Mater.*, 2021, **31**, 2100338, DOI: **10.1002/adfm.202100338**.

30 M. Barnes, S. M. Sajadi, S. Parekh, M. M. Rahman, P. M. Ajayan and R. Verduzco, Reactive 3D Printing of Shape-Programmable Liquid Crystal Elastomer Actuators, *ACS Appl. Mater. Interfaces*, 2020, **12**, 28692–28699, DOI: **10.1021/acsami.0c07331**.

31 A. Kotikian, R. L. Truby, J. W. Boley, T. J. White and J. A. Lewis, 3D Printing of Liquid Crystal Elastomeric Actuators with Spatially Programed Nematic Order, *Adv. Mater.*, 2018, **30**, 1706164, DOI: **10.1002/adma.201706164**.

32 B. Bahadur, S. Chandra and N. K. Sanyal, Phase transition studies of the liquid crystal n-(p-Octyloxybenzylidene)-p-Toluidine, *Phys. Status Solidi A*, 1976, **35**, 387–390, DOI: **10.1002/pssa.2210350142**.

33 S. Schuhladen, F. Preller, R. Rix, S. Petsch, R. Zentel and H. Zappe, Iris-Like Tunable Aperture Employing Liquid-Crystal Elastomers, *Adv. Mater.*, 2014, **26**, 7247–7251, DOI: **10.1002/adma.201402878**.

34 A. Buguin, M.-H. Li, P. Silberzan, B. Ladoux and P. Keller, Micro-Actuators: When Artificial Muscles Made of Nematic Liquid Crystal Elastomers Meet Soft Lithography, *J. Am. Chem. Soc.*, 2006, **128**, 1088–1089, DOI: **10.1021/ja0575070**.

35 S. Li, G. Librandi, Y. Yao, A. J. Richard, A. Schneider-Yamamura, J. Aizenberg and K. Bertoldi, Controlling Liquid Crystal Orientations for Programmable Anisotropic Transformations in Cellular Microstructures, *Adv. Mater.*, 2021, **33**, 2105024, DOI: **10.1002/adma.202105024**.

36 Y. Yao, J. T. Waters, A. V. Shneidman, J. Cui, X. Wang, N. K. Mandsberg, S. Li, A. C. Balazs and J. Aizenberg, Multiresponsive polymeric microstructures with encoded predetermined and self-regulated deformability, *Proc. Natl. Acad. Sci. U. S. A.*, 2018, **115**, 12950–12955, DOI: **10.1073/pnas.1811823115**.

37 M. Tabrizi, T. H. Ware and M. R. Shankar, Voxelated Molecular Patterning in Three-Dimensional Freeforms, *ACS Appl. Mater. Interfaces*, 2019, **11**, 28236–28245, DOI: **10.1021/acsami.9b04480**.

38 Y. Yu, T. Maeda, J. Mamiya and T. Ikeda, Photomechanical Effects of Ferroelectric Liquid-Crystalline Elastomers Containing Azobenzene Chromophores, *Angew. Chem., Int. Ed.*, 2007, **46**, 881–883, DOI: **10.1002/anie.200603053**.

39 A. Münchinger, V. Hahn, D. Beutel, S. Woska, J. Monti, C. Rockstuhl, E. Blasco and M. Wegener, Multi-Photon 4D Printing of Complex Liquid Crystalline Microstructures by In Situ Alignment Using Electric Fields, *Adv. Mater. Technol.*, 2021, 2100944, DOI: **10.1002/admt.202100944**.

40 C. H. Lee, H. Yoshida, Y. Miura, A. Fujii and M. Ozaki, Local liquid crystal alignment on patterned micrograting structures photofabricated by two photon excitation direct laser writing, *Appl. Phys. Lett.*, 2008, **93**, 173509, DOI: **10.1063/1.2952765**.

41 H. Shahsavan, A. Aghakhani, H. Zeng, Y. Guo, Z. S. Davidson, A. Priimagi and M. Sitti, Bioinspired underwater locomotion of light-driven liquid crystal gels, *Proc. Natl. Acad. Sci. U. S. A.*, 2020, **117**, 5125–5133, DOI: **10.1073/pnas.1917952117**.

42 J. A. Castellano, Surface Anchoring of Liquid Crystal Molecules on Various Substrates, *Mol. Cryst. Liq. Cryst.*, 1983, **94**, 33–41, DOI: **10.1080/00268948308084245**.

43 A. K. Tiwari, L. Pattelli, R. Torre and D. S. Wiersma, Remote control of liquid crystal elastomer random laser using external stimuli, *Appl. Phys. Lett.*, 2018, **113**, 013701, DOI: **10.1063/1.5038663**.

44 M. del Pozo, C. Delaney, M. Pilz da Cunha, M. G. Debije, L. Florea and A. P. H. J. Schenning, Temperature-Responsive 4D Liquid Crystal Microactuators Fabricated by Direct Laser Writing by Two-Photon Polymerization, *Small Struct.*, 2021, 2100158, DOI: **10.1002/sstr.202100158**.

45 H. E. Fowler, P. Rothemund, C. Keplinger and T. J. White, Liquid Crystal Elastomers with Enhanced Directional Actuation to Electric Fields, *Adv. Mater.*, 2021, 2103806, DOI: **10.1002/adma.202103806**.

46 D. L. Thomsen, P. Keller, J. Naciri, R. Pink, H. Jeon, D. Shenoy and B. R. Ratna, Liquid Crystal Elastomers with Mechanical Properties of a Muscle, *Macromolecules*, 2001, **34**, 5868–5875, DOI: **10.1021/ma001639q**.

47 Y. Wang, A. Dang, Z. Zhang, R. Yin, Y. Gao, L. Feng and S. Yang, Repeatable and Reprogrammable Shape Morphing from Photoresponsive Gold Nanorod/Liquid Crystal Elastomers, *Adv. Mater.*, 2020, **32**, 2004270, DOI: **10.1002/adma.202004270**.

48 J. J. Wie, K. M. Lee, T. H. Ware and T. J. White, Twists and Turns in Glassy, Liquid Crystalline Polymer Networks, *Macromolecules*, 2015, **48**, 1087–1092, DOI: **10.1021/ma502563q**.

49 Z. He, Y.-H. Lee, F. Gou, D. Franklin, D. Chanda and S.-T. Wu, Polarization-independent phase modulators enabled by two-photon polymerization, *Opt. Express*, 2017, **25**, 33688, DOI: **10.1364/OE.25.033688**.

50 H. Zeng, P. Wasylczyk, G. Cerretti, D. Martella, C. Parmeggiani and D. S. Wiersma, Alignment engineering in liquid crystalline elastomers: Free-form microstructures with multiple functionalities, *Appl. Phys. Lett.*, 2015, **106**, 111902, DOI: **10.1063/1.4915268**.

51 T. H. Ware, M. E. McConney, J. J. Wie, V. P. Tondiglia and T. J. White, Voxelated liquid crystal elastomers, *Science*, 2015, **347**, 982–984, DOI: **10.1126/science.1261019**.

52 T. Guin, M. J. Settle, B. A. Kowalski, A. D. Auguste, R. V. Beblo, G. W. Reich and T. J. White, Layered liquid crystal elastomer actuators, *Nat. Commun.*, 2018, **9**, 2531, DOI: **10.1038/s41467-018-04911-4**.

53 D. Duffy, L. Cmok, J. S. Biggins, A. Krishna, C. D. Modes, M. K. Abdelrahman, M. Javed, T. H. Ware, F. Feng and M. Warner, Shape programming lines of concentrated Gaussian curvature, *J. Appl. Phys.*, 2021, **129**, 224701, DOI: **10.1063/5.0044158**.

54 H. Zeng, O. M. Wani, P. Wasylczyk, R. Kaczmarek and A. Priimagi, Self-Regulating Iris Based on Light-Actuated Liquid Crystal Elastomer, *Adv. Mater.*, 2017, **29**, 1701814, DOI: **10.1002/adma.201701814**.

55 Z. Wang, Z. Wang, Y. Zheng, Q. He, Y. Wang and S. Cai, Three-dimensional printing of functionally graded liquid crystal elastomer, *Sci. Adv.*, 2020, **6**, eabc0034, DOI: **10.1126/sciadv.abc0034**.

56 L. Ren, B. Li, Y. He, Z. Song, X. Zhou, Q. Liu and L. Ren, Programming Shape-Morphing Behavior of Liquid Crystal Elastomers via Parameter-Encoded 4D Printing, *ACS Appl. Mater. Interfaces*, 2020, **12**, 15562–15572, DOI: **10.1021/acsami.0c00027**.

57 J. A. H. P. Sol, H. Sentjens, L. Yang, N. Grossiord, A. P. H. J. Schenning and M. G. Debije, Anisotropic Iridescence and Polarization Patterns in a Direct Ink Written Chiral Photonic Polymer, *Adv. Mater.*, 2021, **33**, 2103309, DOI: **10.1002/adma.202103309**.

58 W. Liao and Z. Yang, The Integration of Sensing and Actuating based on a Simple Design Fiber Actuator towards Intelligent Soft Robots, *Adv. Mater. Technol.*, 2021, 2101260, DOI: **10.1002/admt.202101260**.

59 D. J. Roach, X. Kuang, C. Yuan, K. Chen and H. J. Qi, Novel ink for ambient condition printing of liquid crystal elastomers for 4D printing, *Smart Mater. Struct.*, 2018, **27**, 125011, DOI: **10.1088/1361-665X/aae96f**.

60 M. O. Saed, C. P. Ambulo, H. Kim, R. De, V. Raval, K. Searles, D. A. Siddiqui, J. M. O. Cue, M. C. Stefan, M. R. Shankar and T. H. Ware, Molecularly-Engineered, 4D-Printed Liquid Crystal Elastomer Actuators, *Adv. Funct. Mater.*, 2019, **29**, 1806412, DOI: **10.1002/adfm.201806412**.

61 A. Kotikian, C. McMahan, E. C. Davidson, J. M. Muhammad, R. D. Weeks, C. Daraio and J. A. Lewis, Untethered soft robotic matter with passive control of shape morphing and propulsion, *Sci. Robot.*, 2019, **4**, eaax7044, DOI: **10.1126/scirobotics.aax7044**.

62 G. E. Bauman, J. M. McCracken and T. J. White, Actuation of Liquid Crystalline Elastomers at or Below Ambient Temperature, *Angew. Chem., Int. Ed.*, 2022, **61**, e202202577, DOI: **10.1002/anie.202202577**.

63 M. Pozo, L. Liu, M. Pilz da Cunha, D. J. Broer and A. P. H. J. Schenning, Direct Ink Writing of a Light-Responsive Underwater Liquid Crystal Actuator with Atypical Temperature-Dependent Shape Changes, *Adv. Funct. Mater.*, 2020, **30**, 2005560, DOI: **10.1002/adfm.202005560**.

64 L. Ceamanos, Z. Kahveci, M. López-Valdeolivas, D. Liu, D. J. Broer and C. Sánchez-Somolinos, Four-Dimensional Printed Liquid Crystalline Elastomer Actuators with Fast Photoinduced Mechanical Response toward Light-Driven Robotic Functions, *ACS Appl. Mater. Interfaces*, 2020, **12**, 44195–44204, DOI: **10.1021/acsami.0c13341**.

65 M. del Pozo, J. A. H. P. Sol, S. H. P. van Uden, A. R. Peeketi, S. J. D. Lugger, R. K. Annabattula, A. P. H. J. Schenning and M. G. Debije, Patterned Actuators via Direct Ink Writing of Liquid Crystals, *ACS Appl. Mater. Interfaces*, 2021, **13**, 59381–59391, DOI: **10.1021/acsami.1c20348**.

66 K. Kim, Y. Guo, J. Bae, S. Choi, H. Y. Song, S. Park, K. Hyun and S. Ahn, 4D Printing of Hygroscopic Liquid Crystal Elastomer Actuators, *Small*, 2021, **17**, 2100910, DOI: **10.1002/smll.202100910**.

67 C. P. Ambulo, M. J. Ford, K. Searles, C. Majidi and T. H. Ware, 4D-Printable Liquid Metal–Liquid Crystal Elastomer Composites, *ACS Appl. Mater. Interfaces*, 2021, **13**, 12805–12813, DOI: **10.1021/acsami.0c19051**.

68 E. C. Davidson, A. Kotikian, S. Li, J. Aizenberg and J. A. Lewis, 3D Printable and Reconfigurable Liquid Crystal Elastomers with Light-Induced Shape Memory via Dynamic Bond Exchange, *Adv. Mater.*, 2020, **32**, 1905682, DOI: **10.1002/adma.201905682**.

69 X. Lu, C. P. Ambulo, S. Wang, L. K. Rivera-Tarazona, H. Kim, K. Searles and T. H. Ware, 4D-Printing of Photoswitchable Actuators, *Angew. Chem., Int. Ed.*, 2021, **60**, 5536–5543, DOI: **10.1002/anie.202012618**.

70 X. Peng, X. Kuang, D. J. Roach, Y. Wang, C. M. Hamel, C. Lu and H. J. Qi, Integrating digital light processing with direct ink writing for hybrid 3D printing of functional structures and devices, *Addit. Manuf.*, 2021, **40**, 101911, DOI: **10.1016/j.addma.2021.101911**.

71 C. Zhang, X. Lu, G. Fei, Z. Wang, H. Xia and Y. Zhao, 4D Printing of a Liquid Crystal Elastomer with a Controllable Orientation Gradient, *ACS Appl. Mater. Interfaces*, 2019, **11**, 44774–44782, DOI: **10.1021/acsami.9b18037**.

72 H. Zeng, D. Martella, P. Wasylczyk, G. Cerretti, J.-C. G. Lavocat, C.-H. Ho, C. Parmeggiani and D. S. Wiersma, High-Resolution 3D Direct Laser Writing for Liquid-Crystalline Elastomer Microstructures, *Adv. Mater.*, 2014, **26**, 2319–2322, DOI: **10.1002/adma.201305008**.

73 S. Nocentini, D. Martella, C. Parmeggiani, S. Zanotto and D. S. Wiersma, Structured Optical Materials Controlled by Light, *Adv. Opt. Mater.*, 2018, **6**, 1800167, DOI: **10.1002/adom.201800167**.

74 L. Chen, Y. Dong, C.-Y. Tang, L. Zhong, W.-C. Law, G. C. P. Tsui, Y. Yang and X. Xie, Development of Direct-Laser-Printable Light-Powered Nanocomposites, *ACS Appl. Mater. Interfaces*, 2019, **11**, 19541–19553, DOI: **10.1021/acsami.9b05871**.

75 K.-W. Yeung, Y. Dong, L. Chen, C.-Y. Tang, W.-C. Law, G. C.-P. Tsui and D. S. Engstrøm, Printability of photo-sensitive nanocomposites using two-photon polymerization, *Nanotechnol. Rev.*, 2020, **9**, 418–426, DOI: **10.1515/ntrev-2020-0031**.

76 Y. Guo, J. Zhang, W. Hu, M. T. A. Khan and M. Sitti, Shape-programmable liquid crystal elastomer structures with arbitrary three-dimensional director fields and geometries, *Nat. Commun.*, 2021, **12**, 5936, DOI: **10.1038/s41467-021-26136-8**.

77 Z. Ji, X. Zhang, B. Shi, W. Li, W. Luo, I. Drevensek-Olenik, Q. Wu and J. Xu, Compartmentalized liquid crystal alignment induced by sparse polymer ribbons with surface relief gratings, *Opt. Lett.*, 2016, **41**, 336, DOI: **10.1364/OL.41.000336**.

78 Y. Guo, H. Shahsavan and M. Sitti, 3D Microstructures of Liquid Crystal Networks with Programmed Voxelated

Director Fields, *Adv. Mater.*, 2020, **32**, 2002753, DOI: **10.1002/adma.202002753**.

79 B. Bahadur, Magnetic susceptibility studies of the liquid crystal, N-(p-hexyloxybenzylidene)-p-toluidine (HBT), *J. Chem. Phys.*, 1977, **67**, 3272–3273.

80 M. Fang, T. Liu, Y. Xu, B. Jin, N. Zheng, Y. Zhang, Q. Zhao, Z. Jia and T. Xie, Ultrafast Digital Fabrication of Designable Architectured Liquid Crystalline Elastomer, *Adv. Mater.*, 2021, **33**, 2105597, DOI: **10.1002/adma.202105597**.

81 D. Joralmon, S. Alfarhan, S. Kim, T. Tang, K. Jin and X. Li, Three-Dimensional Printing of Liquid Crystals with Thermal Sensing Capability via Multimaterial Vat Photopolymerization, *ACS Appl. Polym. Mater.*, 2022, **4**, 2951–2959, DOI: **10.1021/acsapm.2c00322**.

82 Q. He, Z. Wang, Y. Wang, A. Minori, M. T. Tolley and S. Cai, Electrically controlled liquid crystal elastomer–based soft tubular actuator with multimodal actuation, *Sci. Adv.*, 2019, **5**, eaax5746, DOI: **10.1126/sciadv.aax5746**.

83 Y. Zhao, Y. Chi, Y. Hong, Y. Li, S. Yang and J. Yin, Twisting for soft intelligent autonomous robot in unstructured environments, *Proc. Natl. Acad. Sci. U. S. A.*, 2022, **119**, e2200265119, DOI: **10.1073/pnas.2200265119**.

84 Y. Li, C. Luo, K. Yu and X. Wang, Remotely Controlled, Reversible, On-Demand Assembly and Reconfiguration of 3D Mesostructures via Liquid Crystal Elastomer Platforms, *ACS Appl. Mater. Interfaces*, 2021, **13**, 8929–8939, DOI: **10.1021/acsami.0c21371**.

85 H. Liu, H. Tian, X. Li, X. Chen, K. Zhang, H. Shi, C. Wang and J. Shao, Shape-programmable, deformation-locking, and self-sensing artificial muscle based on liquid crystal elastomer and low–melting point alloy, *Sci. Adv.*, 2022, **8**, eabn5722.

86 J. Lv, Y. Liu, J. Wei, E. Chen, L. Qin and Y. Yu, Photocontrol of fluid slugs in liquid crystal polymer microactuators, *Nature*, 2016, **537**, 179–184, DOI: **10.1038/nature19344**.

87 Y. Wang, W. Liao, J. Sun, R. Nandi and Z. Yang, Bioinspired Construction of Artificial Cardiac Muscles Based on Liquid Crystal Elastomer Fibers, *Adv. Mater. Technol.*, 2022, **7**, 2100934, DOI: **10.1002/admt.202100934**.

88 D. J. Roach, C. Yuan, X. Kuang, V. C.-F. Li, P. Blake, M. L. Romero, I. Hammel, K. Yu and H. J. Qi, Long Liquid Crystal Elastomer Fibers with Large Reversible Actuation Strains for Smart Textiles and Artificial Muscles, *ACS Appl. Mater. Interfaces*, 2019, **11**, 19514–19521, DOI: **10.1021/acsami.9b04401**.

89 H. Zeng, P. Wasylczyk, C. Parmeggiani, D. Martella, M. Burresi and D. S. Wiersma, Light-Fueled Microscopic Walkers, *Adv. Mater.*, 2015, **27**, 3883–3887, DOI: **10.1002/adma.201501446**.

90 M. Zhang, H. Shahsavan, Y. Guo, A. Pena-Francesch, Y. Zhang and M. Sitti, Liquid-Crystal-Elastomer-Actuated Reconfigurable Microscale Kirigami Metastructures, *Adv. Mater.*, 2021, 2008605.

91 M. del Pozo, C. Delaney, C. W. M. Bastiaansen, D. Diamond, A. P. H. J. Schenning and L. Florea, Direct Laser Writing of Four-Dimensional Structural Color Microactuators Using a Photonic Photoresist, *ACS Nano*, 2020, **14**, 9832–9839, DOI: **10.1021/acsnano.0c02481**.

92 M. López-Valdeolivas, D. Liu, D. J. Broer and C. Sánchez-Somolinos, 4D Printed Actuators with Soft-Robotic Functions, *Macromol. Rapid Commun.*, 2018, **39**, 1700710, DOI: **10.1002/marc.201700710**.

93 Z. Jiang, M. Xu, F. Li and Y. Yu, Red-Light-Controllable Liquid-Crystal Soft Actuators via Low-Power Excited Upconversion Based on Triplet–Triplet Annihilation, *J. Am. Chem. Soc.*, 2013, **135**, 16446–16453, DOI: **10.1021/ja406020r**.

94 H. Tian, Z. Wang, Y. Chen, J. Shao, T. Gao and S. Cai, Polydopamine-Coated Main-Chain Liquid Crystal Elastomer as Optically Driven Artificial Muscle, *ACS Appl. Mater. Interfaces*, 2018, **10**, 8307–8316, DOI: **10.1021/acsami.8b00639**.

95 M. Zadan, D. K. Patel, A. P. Sabelhaus, J. Liao, A. Wertz, L. Yao and C. Majidi, Liquid Crystal Elastomer with Integrated Soft Thermoelectrics for Shape Memory Actuation and Energy Harvesting, *Adv. Mater.*, 2022, **34**, 2200857, DOI: **10.1002/adma.202200857**.